

MEASURED ANOMALOUS RADAR PROPAGATION AND OCEAN BACKSCATTER IN THE VIRGINIA COASTAL REGION

Janet K. Stapleton, V. Russell Wiss, Robert E. Marshall,
Naval Surface Warfare Center, Dahlgren, VA

1. INTRODUCTION

In the spring of 2000, the Office of Naval Research (ONR) sponsored experiments to characterize the effects of low altitude refraction on the propagation of microwave signals. In specific these experiments were focused on the performance of shipboard Navy radars in terms of the signal levels returned from targets as well as clutter sources, Stapleton (2001). The location of the experiments off the coast of Wallops Island VA, stressed the impact of the land / sea interface in the phenomena observed. These littoral settings are of increasing importance to the Navy's mission and have proven to be challenging for the performance of Navy radars. The experiments showed that this environment is also very dynamic in both the spatial and temporal dimensions. Microwave emitters operating in similar geometries and elevation angles including radar, communications, and telemetry systems would be subject to the phenomena observed.

2. EXPERIMENT SCENARIOS

The experiments involved the sensing of meteorological parameters known to drive refractivity, direct measurements of pathloss at microwave frequencies in the S, C, and X bands, and S band radar returns from sea surface clutter. These measurements were conducted simultaneously to the degree possible, since one aspect of the experiment was to gain insight into the temporal variability of refractivity and its effect on the radar pathloss and clutter backscatter.

2.1. Refractivity Measurements

Refractivity was derived from a variety of meteorological sources including the Johns Hopkins Applied Physics Laboratory helicopter sensing system, which allowed the collection of range and height dependent profiles of temperature, humidity, and pressure via a sawtooth flight pattern. Bulk measurements of temperature, humidity, pressure, and wind speed were collected throughout the experiments at several locations

including the shoreline and at buoy and boat sites over the water. The bulk measurements allowed the estimation of evaporation duct profiles, which are known to be prevalent in maritime environments. On some occasions including those when the helicopter measurements were unavailable, rocket sondes were used to collect refractivity profile data over the water at fixed boat locations.

2.2. Pathloss Measurements

During these experiments, a unique approach was taken to measuring pathloss via a set of vertically scanning CW transmitters onboard a boat and a complimentary set of receivers at the high water line on shore. These measurements were made simultaneously at S, C and X bands as the boat traversed outbound from 6 km to 56 km from shore. Using careful calibration for both receivers and transmitters, the pathloss measured was converted to propagation factor relative to freespace spreading loss and coverage diagrams of the same were created. The propagation coverage diagrams were produced for the ranges mentioned from 1 to 10 m above the surface based on a receiver at 20 to 30 m above mean water level, depending on the frequency selected. This representation of the propagation factor allowed for easy comparison with propagation model outputs based on the refractivity data collected in the same region and over the same time periods. An example of one such coverage diagram comparison chart appears in Figure 2.2-1 below. (The original figure was color-coded. This representation is in grayscale for purposes of this publication.)

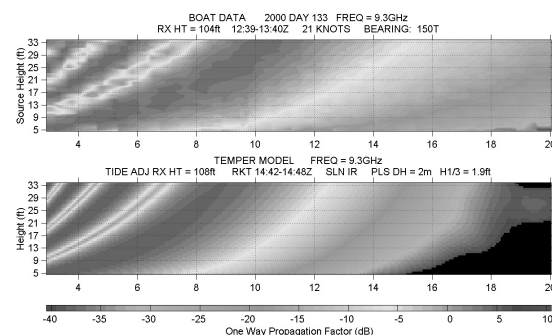


**Figure 2.2-1 Measured and Modeled X band
Propagation Coverage Diagrams**

* Corresponding author address: Janet K. Stapleton, Naval Surface Warfare Center, Photonics Systems and Technology Branch T44, Dahlgren, VA 22448; e-mail stapletonjk@nswc.navy.mil

2.3. Radar Sea Clutter Measurements

Radar sea surface clutter measurements were also collected simultaneously with the meteorological, refractivity and pathloss data. Previous observations of sea surface backscatter had shown a tight coupling of surface backscatter levels as well as the spatial relationships (ranges and azimuths of intense returns) with the existence of non-standard or anomalous propagation. Therefore the hope was to capture the change in sea surface return along with the associated change in meteorology and measured propagation losses. The sea surface backscatter was collected using both the SPANDAR atmospheric research radar and the AN/SPY-1A both resident at Wallops Island VA. The two systems had different limitations in the spatial and temporal rates for data collection. The SPANDAR data was collected over 180 deg azimuth and out to 270 km range, at an update rate of 15 min. The AN/SPY-1A data was collected over a 60 deg azimuth sector and to approximately 55 km range, with an update rate of 3 min. The time sequences of clutter return levels over these sectors allowed display of the clutter variation in range and azimuth as a function of the time between images. In this way the temporal scale of the changes in the coupled sea surface / propagation environment could be observed up to the sampling interval.

3. OBSERVATIONS

The following sections show examples of the various phenomena observed during the experiments. The TEMPER (Tropospheric ElectroMagnetic Parabolic Equation Routine) developed by Johns Hopkins Applied Physics, was used to model the expected propagation loss based on meteorological refractivity measurements, Dockery (1988). This model accepts sequences of range dependent refractivity data as input, as well as single profile data. Figure 2.2-1 includes a TEMPER output coverage diagram in the lower panel. This result was based on a single rocket sonde refractivity profile and an estimate of the evaporation duct profile using boat meteorological measurements.

3.1. Spatial Variability

Quantifying the spatial variation of the refractivity, propagation and sea surface return was a goal of the experiment. The dynamic nature of the coastal environment, as well as the practical logistic limitations of the measurement systems were limiting factors in achieving this goal. The radar clutter returns showed some of the best illustrations of the spatial variations, where large differences in character were observed both with azimuth angle and range. The refractivity profile sequences from the helicopter and the repetitive

measurements of pathloss versus range also provided insight; however these measurements were made using relatively slow platforms (compared to the speed of a microwave signal); a boat at 10 m/s and a helicopter at 30 m/s. In some cases the total time to traverse the 50 km path was over one hour, and the observed temporal changes in clutter and measured pathloss occurred within the measurement period. In this way the temporal and spatial variations observed were not completely separable. Figure 3.1-1 shows the refractivity versus range as sensed by the helicopter measurement system. The change in the duct height versus range is reflected by the change in the vertical position of the negatively sloping section of the profiles. Figure 3.1-2 shows the resultant measured and modeled propagation coverage diagrams for this event at S band. Notice the large convergence zone shown by the higher propagation factor values beyond 20 nmi range. At this location, the S band radars also produced a strong increase in sea clutter backscatter level.

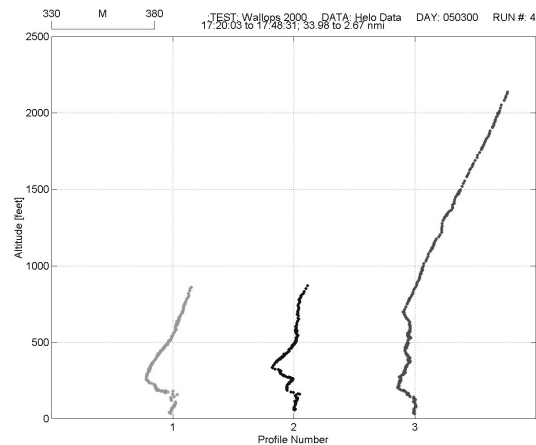


Figure 3.1-1 Helicopter Modified Refractivity Profiles versus Range

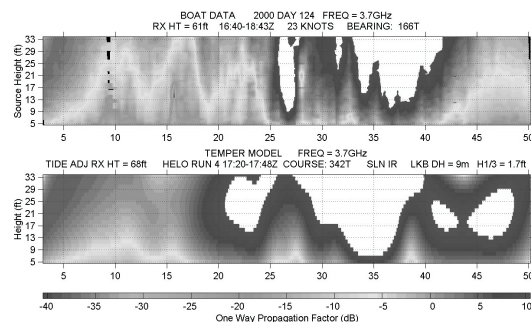


Figure 3.1-2 Measured and Modeled S Band Propagation Coverage Diagrams

3.2. Temporal Variability

The temporal variations of the propagation environment were also of keen interest during the experiments. This information would help define the update rates required for either test or operational Navy assessments of the environment. Again subject to the limitations in the update rates of the measurement systems, we were able to determine that under some conditions, the environment was quite stationary with the observed changes in refractivity, pathloss, and clutter being gradual and of smaller magnitude. However during some events, large variations were evident at the sampling rate of our sensors. Hence, we could not determine the true scale of these fluctuations, but only that they were at least at the measurement rate. Figures 3.2-1 through 3.2-4 show the time sequence of two pathloss measurement events and the refractivity sensed during these same periods.

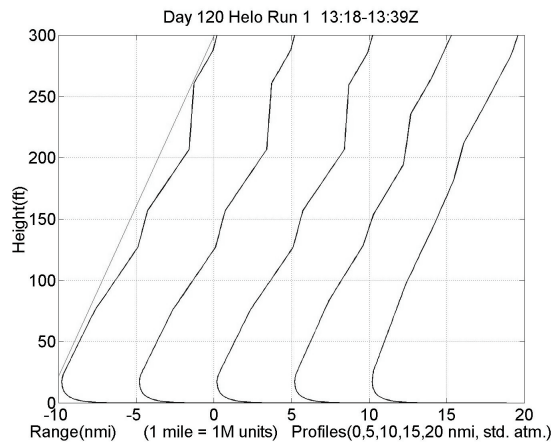


Figure 3.2-1 Helicopter Modified Refractivity versus Range 13:18Z

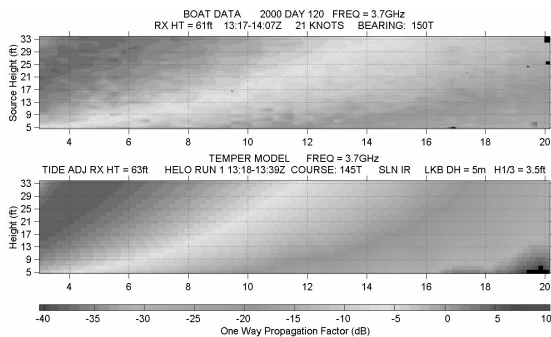


Figure 3.2-2 Measured and Modeled Propagation Coverage Diagram 13:17Z

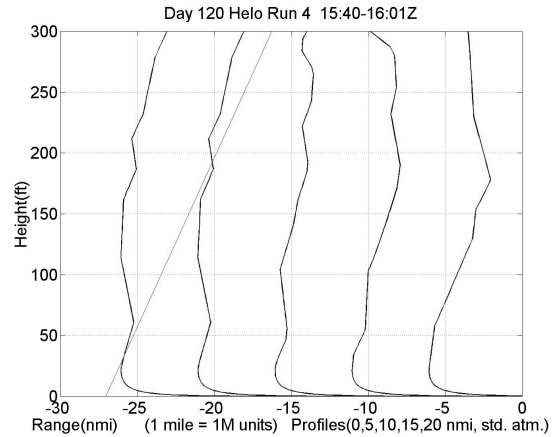


Figure 3.2-3 Helicopter Modified Refractivity versus Range 15:40Z

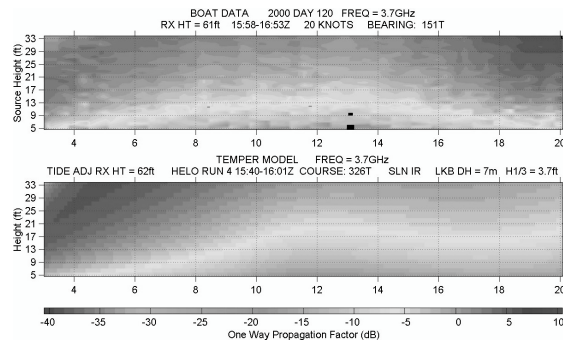


Figure 3.2-4 Measured and Modeled S Band Propagation Coverage Diagram 15:58Z

4. IMPLICATIONS

These experiments produced a wealth of data, which is still being analyzed and understood as to the sources of the variations observed, and the implications for various types of systems employing low angle microwave emitters. The results have shown that the Mid-Atlantic coastal region provides a challenging and dynamic environment in both the spatial and temporal domains. Changes on the order of 25 dB in one way propagation loss were observed in less than 10 minutes time, and over less than 1 meter vertically and 1 km range. For a radar this change would equate to a 50 dB two way signal level change and subsequent error in assumed radar cross section for an observed scatterer. Clearly the temporal and spatial scale of these variations also challenges those beset with the task of collecting sufficient ground truth or calibration data for determining propagation adjusted radar return power levels.

5. REFERENCES

Dockery, G. D., 1988: Modeling Electromagnetic Wave Propagation in the Troposphere Using the Parabolic Equation. *IEEE Trans. Antenna Propag.* 36(10), 1464-1470.

Stapleton, J. K., 2001: Radar Propagation Modeling Assessment Using Measured Refractivity and Directly Sensed Propagation Ground Truth – Wallops Island, VA 2000. NSWCCD/TR-01/132.